firing gave predominantly superconducting material, with small amounts of impurity phases. This synthetic route to superconducting $YBa_2Cu_3O_{7-\delta}$ was not pursued further because of two limitations: (1) the inability to solubilize the copper ethylene glycol salt via complexation with barium in the desired 3:2 Cu:Ba stoichiometry, and (2) the lack of a suitable yttrium alkoxide which is soluble in ethylene glycol.

Acknowledgment. This research was sponsored by the National Science Foundation (Grant DMR-8716255). Acknowledgment is also made to the donors of the Petroleum Research Fund, administered by the American Chemical Society, for partial support of this research. We thank W. Marshall for the X-ray data collection.

Supplementary Material Available: Tables giving full crystallographic information, positional parameters, anisotropic thermal parameters, hydrogen atom parameters, and interatomic distances and angles for the two compounds (15 pages); listings of observed and calculated structure factors for the two compounds (16 pages). Ordering information is given on any current masthead page.

Contribution from the Department of Chemistry and Center for Superconductivity Research, University of Maryland, College Park, Maryland 20742, and Department of Chemistry, Purdue University, West Lafayette, Indiana 47907

Synthesis and Structure of $Ba_6Hf_5S_{16}$ and $Ba_5Hf_4S_{13}$: The n = 5 and 4 Members of the $A_{n+1}B_nX_{3n+1}$ Ruddlesden-Popper Phases

Bai-Hao Chen,[†] Bryan W. Eichhorn,*[,†] and Philip E. Fanwick[‡]

Received November 27, 1991

Two new Ba/Hf/S phases of formula $Ba_5Hf_4S_{13}$ and $Ba_6Hf_5S_{16}$ have been prepared from BaS, Hf, and elemental sulfur at 1050 °C in $BaCl_2$ flux reactions. The compounds are the n = 4 and 5 members of the $Ba_{n+1}Hf_nS_{3n+1}$ series which are rare examples of Ruddlesden-Popper sulfides. The compounds contain perovskite blocks extending infinitely in a and b with double BaS layers and a $0\ ^1/_2\ 0$ shift every n layers in c. The Hf-S distances in both compounds average 2.48 (2) Å with regular HfS_6 octahedra. The 12-coordinate Ba atoms display Ba-S distances averaging 3.49 (2) Å with the Ba-S distances for the 9-coordinate Ba atoms in the double BaS layers ranging between 3.08 and 3.52 Å. Crystal data for $Ba_5Hf_4S_{13}$ (20 °C): a = 6.977 (1) Å, b = 7.006 (2) Å, and c = 45.280 (5) Å, Z = 4, D_{calc} = 5.45 g/cm³, orthorhombic, space group *Fmmm*. Crystal data for $Ba_6Hf_5S_{16}$ (20 °C): a = 7.002 (1) Å, b = 6.987 (2) Å, and c = 55.205 (6) Å, Z = 4, D_{calc} = 5.48 g/cm³, orthorhombic, space group *Fmmm*.

Introduction

The oxides of general formula $A_{n+1}B_nO_{3n+1}$, first identified in the Sr/Ti/O system by Ruddlesden and Popper,[1] represent an important class of solid-state materials. The most well-known structures in the series are the n = 1 members, which have the K_2NiF_4 structure type, and the n = ∞ compounds, which are the ABO_3 perovskites.[2] Intermediate phases with n = 2, 3 are known for the group 4 oxides,[1,3,4] the strontium and europium vanadium oxides,[5-7] and the $La_{2-x}Sr_xCaCu_2O_6$ copper oxides[8] to name a few.[9] The copper-oxide phases are high-temperature superconductors with transition temperatures as high as 60 K.[10] In an attempt to extend the Ruddlesden-Popper phases into the metal sulfides, we[11] and others[12] have recently reported the preparation of the Ba_2MS_4 (n = 1; M = Hf and Zr) and $Ba_3Zr_2S_7$ (n = 2) phases. We report here the synthesis, structure, and properties of $Ba_5Hf_4S_{13}$ (n = 4) and $Ba_6Hf_5S_{16}$ (n = 5) that, together with $BaHfS_3$ (n = ∞),[13] are the third and fourth Ba-Hf-S phases characterized to date. To our knowledge, these compounds are the first $A_{n+1}B_nX_{3n+1}$ phase with n > 3 to be structurally characterized (excluding n = ∞).

Experimental Section

General Procedures. All sample manipulations were conducted in a Vacuum Atmospheres Co. drybox system. All reagents were purchased from Cerac Inorganics and used as received. Powder X-ray data were collected on a modified Phillips XRG 2000 diffractometer interfaced with a Radix databox and MDI software system.

Synthesis of $Ba_5Hf_4S_{13}$ and $Ba_6Hf_5S_{16}$. BaS, Hf powder, and elemental sulfur in a 3:2:4 ratio, respectively, were ground and loaded into a silica ampule along with 25% $BaCl_2$ by weight. The tube was sealed under vacuum and placed inside a larger silica tube which was also sealed under vacuum. The material was heated to 1050 °C at 0.3 °C/min and fired at 1050 °C for an additional 20 h. The sample was then quickly cooled to room temperature ($^1/_2$ h.). The resulting material was washed with water to dissolve the $BaCl_2$ flux, leaving two types of well-formed crystals: orange-brown plates and darker brown parallelepipeds. A lighter orange-brown powder primarily composed of elemental sulfur and some BaS was also present. The single crystals accounted for ca. 70% of the reaction mixture. The synthesis is reproducible.

Table I. Summary of Crystallographic Data for $Ba_5Hf_4S_{13}$ and $Ba_6Hf_5S_{16}$

	$Ba_5Hf_4S_{13}$	$Ba_6Hf_5S_{16}$
fw	1817.49	2229.51
space group	*Fmmm*	*Fmmm*
cell dimens at 20 °C		
a, Å	6.977 (1)	7.002 (1)
b, Å	7.006 (2)	6.987 (2)
c, Å	42.280 (5)	55.205 (6)
V, Å³	2213 (1)	2700 (1)
Z	4	4
linear abs coeff, cm⁻¹	284.35	287.53
rel. transm factors: max; min	1.0; 0.59	1.0; 0.09
no. of unique data	757	541
data with $I > 3.0\sigma(I)$	686	469
no. of variables	42	49
shift/esd final cycle	0.01	0.27
$R(F_o)^a$	0.054	0.079
$R_w(F_o)^a$	0.085	0.130
density, g/cm³	5.45	5.48

$^a R(F_o) = \sum|F_o - F_c|/\sum F_o$; $R_w(F_o) = (\sum w|F_o - F_c|^2/\sum wF_o^2)^{1/2}$.

[†] University of Maryland.
[‡] Purdue University.

(1) Ruddlesden, S. N.; Popper, P. *Acta Crystallogr.* **1958**, *11*, 54.
(2) Wells, A. F. *Structural Inorganic Chemistry*, 5th ed.; Clarendon Press: Oxford, England; 1986.
(3) Elcombe, M. M.; Kisi, E. H.; Hawkins, K. D.; White, T. J.; Goodman, P.; Matheson, S. *Acta Crystallogr.* **1991**, *B47*, 305.
(4) Blasse, G. *J. Inorg. Nucl. Chem.* **1968**, *30*, 656.
(5) Gong, W.; Xue, J. S.; Greedan, J. E. *J. Solid State Chem.* **1991**, *91*, 180.
(6) McCarthy, G. J.; White, W. B.; Roy, R. *J. Inorg. Nucl. Chem.* **1969**, *31*, 329.
(7) Itoh, M.; Shikano, M.; Liang, R.; Kawaji, H.; Nakamura, T. *J. Solid State Chem.* **1990**, *88*, 597.
(8) Nguyen, N.; Er-Rakho, L.; Michel, C.; Choisnet, J.; Raveau, B. *Mater. Res. Bull.* **1980**, *15*, 891.
(9) (a) Nomura, S. *Landolt-Bornstein*; Springer-Verlag: Berlin, 1978; Group III/12a, p 425. (b) Goodenough, J. B.; Longo, J. M. *Landolt-Bornstein*; Springer-Verlag: Berlin, 1970; Group III/4a, p 126.

0020-1669/92/1331-1788$03.00/0

Crystallographic Studies. Structural Determination of $Ba_5Hf_4S_{13}$. A dark brown brick of dimensions 0.28 × 0.1 × 0.1 mm was mounted on a glass fiber in a random orientation. Data collection was performed at 20 °C with Mo Kα radiation (λ = 0.71073 Å) on an Enraf-Nonius CAD4 computer-controlled κ-axis diffractometer equipped with a graphite crystal, incident beam monochromator.

Cell constants and an orientation matrix for data collection were obtained from least-squares refinement, using setting angles of 25 reflections in the range $26 < \theta < 28°$, measured by the computer-controlled diagonal slit method of centering. The crystallographic data are summarized in Table I. A total of 757 unique reflections were collected between 4° and 55° in 2θ with 686 having $I \geq (3\sigma)I$. The latter were used in refinement of the structure. Lorentz and polarization corrections were applied to the data. An empirical absorption correction[14] and a secondary extinction correction[15] were applied. Scattering factors and anomalous dispersion corrections were taken from refs 16 and 17, respectively.

The data were indexed on a face-centered orthorhombic cell and displayed no additional systematic absences, consistent with space groups *F*222, *Fmm*2, and *Fmmm*. Solution and refinement in the higher symmetry space group *Fmmm* (No. 69) confirmed the latter as the correct choice. The initial atom coordinates were estimated using idealized positions based on a standard Ruddlesden–Popper type structure. The structure was successfully refined (SHELX-86) by the full-matrix least-squares method with all atoms anisotropic in the final cycles. The final residuals were $R(F_o) = 5.4\%$ and $R_w(F_o) = 8.5\%$. The highest peak in the final difference map was 4.17 e/Å^3.

Structural Determination of $Ba_6Hf_5S_{16}$. An orange-brown plate of approximate dimensions of 0.17 × 0.17 × 0.04 mm was mounted on a glass fiber in a random orientation. Data were collected at 20 °C as described above. Cell constants and an orientation matrix for data collection were obtained from least-squares refinement, using setting angles of 25 reflections in the range $21 < \theta < 23°$. Data were collected in plate mode from 4 to 45° in 2θ by using the ω scan technique. A total of 541 unique reflections were collected of which 469 having $I \geq 3\sigma(I)$ were used in solution and refinement. Lorentz and polarization corrections were applied. Due to the platelike nature of the crystals, significant absorption problems existed as evidenced by the relative transmission factors of 1.000 (maximum) and 0.091 (minimum). An empirical absorption correction[14] and a secondary extinction correction[15] were applied. Scattering factors and anomalous dispersion corrections were taken from refs 16 and 17, respectively.

The data were indexed on a face-centered orthorhombic cell and displayed no additional systematic absences, consistent with space groups *F*222, *Fmm*2, and *Fmmm*. Solution and refinement in the higher symmetry space group *Fmmm* (No. 69) confirmed the latter as the correct choice. The structure was solved by using SHELX-86. The remaining atoms were located in the succeeding difference Fourier syntheses. The structure was successfully refined by the full-matrix least-squares method with all atoms aniostropic in the final cycles. The final residuals were $R(F_o) = 7.9\%$ and $R_w(F_o) = 13.0\%$. The highest peak in the final difference Fourier had a height of 4.02 e/Å^3.

Results and Discussion

In an attempt to prepare single crystals of the $Ba_3Hf_2S_7$ phase, BaS, Hf powder, and elemental sulfur in a 3:2:4 ratio, respectively, were ground and loaded into a silica ampule along with $BaCl_2$ (25 wt %) to aid in crystal growth. After the ampule was heated to 1050 °C, the $BaCl_2$ was washed away with water leaving an equal mixture of orange-brown plates ($Ba_6Hf_5S_{16}$) and darker brown parallelepipeds ($Ba_5Hf_4S_{13}$), which together accounted for ca. 70% of the total product mass. The EDAX analysis on both types of single crystals showed Ba, Hf, and S but did not show the presence of Cl, indicating that chloride incorporation from the flux was negligible. It was not possible to separate the two types of crystals manually or prepare them as individual single-phase compounds. Ceramic preparations of the compounds in the absence of $BaCl_2$ showed mixtures of both $Ba_6Hf_5S_{16}$ and $Ba_5Hf_4S_{13}$ along with the possible presence of other $Ba_{n+1}Hf_nS_{3n+1}$ phases. Because the structures of both compounds are composed of offset perovskite slabs (see below), the calculated and observed powder X-ray diffraction (PXRD) profiles closely resemble that of the $BaHfS_3$ perovskite. Thus, distinguishing between the two phases, or any $Ba_{n+1}Hf_nS_{3n+1}$ phase with $n > 4$, is difficult by PXRD.

The single-crystal X-ray data set for $Ba_6Hf_5S_{16}$ was indexed on a face-centered orthorhombic cell [$a = 7.002$ (1) Å, $b = 6.987$ (2) Å, and $c = 55.205$ (6) Å] and successfully refined in space group *Fmmm*. A summary of the crystallographic data and the fractional coordinates are given in Tables I and II, respectively. Selected bond distances and angles are given in Table III. Due to absorption problems associated with the platelike nature of the crystal, the final residuals were high with $R(F_o) = 7.9\%$ and $R_w(F_o) = 13\%$. A higher symmetry tetragonal cell with *I*4/*mmm* symmetry was discounted due to the following reasons: (1) the (001) faces of indexed thin plates extinguished under a polarizing light microscope which is inconsistent with a tetragonal cell, and (2) three independent searches (on two different diffractometers) of reciprocal space yielded reflections that were indexed on the same orthorhombic cell. Attempted solutions and refinements of the data in *I*4/*mmm* and other space groups were unsuccessful. The X-ray data set for $Ba_5Hf_4S_{13}$ was also indexed on a face-centered orthorhombic cell [$a = 6.977$ (1) Å, $b = 7.006$ (2) Å, and $c = 45.280$ (5) Å] and successfully refined in space group *Fmmm* with final residuals of 5.4% and 8.5% for $R(F_o)$ and $R_w(F_o)$, respectively. The crystallographic data for $Ba_5Hf_4S_{13}$ are

Table II. Fractional Coordinates and Isotropic Thermal Parameters for $Ba_6Hf_5S_{16}$

atom	*x*	*y*	*z*	B,[a] Å^2
Hf(1)	0	0	0	0.53 (6)
Hf(2)	0	0	0.09003 (4)	0.43 (4)
Hf(3)	0	0	0.18095 (4)	0.75 (4)
Ba(1)	1/2	0	0.04501 (6)	2.64 (9)
Ba(2)	1/2	0	0.13445 (6)	1.31 (7)
Ba(3)	1/2	0	0.21847 (6)	1.50 (7)
S(1)	0	0	0.0448 (3)	4.5 (6)
S(2)	0	0	0.1352 (3)	4.7 (5)
S(3)	0	0	0.2256 (3)	2.1 (3)
S(4)	1/4	1/4	0.1788 (2)	2.7 (2)
S(5)	1/4	1/4	0.0901 (3)	7.0 (4)
S(6)	1/4	1/4	0	7.2 (7)

[a] Values for anisotropically refined atoms are given in the form of the isotropic equivalent thermal parameter defined as (4/3) $[a^2\beta(1,1) + b^2\beta(2,2) + c^2\beta(3,3) + ab(\cos\gamma)\beta(1,2) + ac(\cos\beta)\beta(1,3) + bc(\cos\alpha)\beta(2,3)]$.

Table III. Selected Bond Distances (Å) and Angles (deg) for $Ba_6Hf_5S_{16}$

Hf(1)–S(1)	2.47 (2)	Ba(1)–S(5)	3.51 (1)
Hf(1)–S(6)	2.473 (1)	Ba(1)–S(6)	3.506 (3)
Hf(2)–S(1)	2.50 (2)	Ba(2)–S(2)	3.501 (1)
Hf(2)–S(2)	2.49 (2)	Ba(2)–S(2)	3.494 (1)
Hf(2)–S(5)	2.473 (1)	Ba(2)–S(4)	3.48 (1)
Hf(3)–S(2)	2.53 (2)	Ba(2)–S(5)	3.48 (1)
Hf(3)–S(3)	2.47 (2)	Ba(3)–S(3)	3.523 (2)
Hf(3)–S(4)	2.476 (2)	Ba(3)–S(3)	3.09 (2)
Ba(1)–S(1)	3.501 (1)	Ba(3)–S(3)	3.516 (2)
Ba(1)–S(1)	3.494 (1)	Ba(3)–S(4)	3.30 (1)
S(1)–Hf(1)–S(1)	180.00	S(1)–Ba(1)–S(1)	90.0 (2)
S(1)–Hf(1)–S(6)	90.00	S(1)–Ba(1)–S(5)	60.2 (3)
S(6)–Hf(1)–S(6)	90.00	S(1)–Ba(1)–S(1)	180 (2)
S(1)–Hf(2)–S(5)	90.0 (4)	S(2)–Hf(3)–S(4)	87.3 (3)
S(2)–Hf(2)–S(5)	90.0 (4)	S(3)–Hf(3)–S(4)	92.7 (3)
S(5)–Hf(2)–S(5)	180 (1)	S(4)–Hf(3)–S(4)	174.5 (7)
S(5)–Ba(1)–S(5)	59.7 (3)	S(2)–Ba(2)–S(2)	178.7 (7)
S(3)–Ba(3)–S(3)	83.6 (3)	S(3)–Ba(3)–S(4)	63.1 (3)
S(3)–Ba(3)–S(4)	126.9 (2)	S(2)–Ba(2)–S(4)	59.3 (3)
S(3)–Ba(3)–S(3)	167.2 (6)	S(2)–Ba(2)–S(5)	60.3 (3)
S(2)–Ba(2)–S(5)	120.7 (3)		

(10) Cava, R. J.; Batlogg, B.; van Dover, R. B.; Krajewski, J. J.; Waszczak, J. V.; Fleming, R. M.; Peck, W. F., Jr.; Rupp, L. W., Jr.; Marsh, P.; James, A. C. W. P.; Schneemeyer, L. F. *Nature* **1990**, *345*, 602.
(11) Chen, B.-H.; Eichhorn, B. W. *Mater. Res. Bull.* **1991**, *26*, 1035.
(12) Saeki, M.; Yafima, Y.; Onoda, M. *J. Solid State Chem.* **1991**, *92*, 286.
(13) Lelieveld, R.; Ijdo, D. J. *Acta Crystallogr.* **1980**, *B36*, 2223.
(14) Walker, N.; Stuart, D. *Acta Crystallogr.* **1983**, *A39*, 158.
(15) Zachariasen, W. H. *Acta Crystallogr.* **1963**, *16*, 1139.
(16) Cromer, D. T.; Waber, J. T. *International Tables for X-Ray Crystallography*; The Kynoch Press: Birmingham, England, 1974; Vol. IV, Table 2.2B.
(17) Ibers, J. A.; Hamilton, W. C. *Acta Crystallogr.* **1964**, *17*, 781.

Table IV. Fractional Coordinates and Isotropic Thermal Parameters for $Ba_5Hf_4S_{13}$

atom	x	y	z	B,[a] Å^2
Hf(1)	0	0	0.05496 (2)	0.46 (2)
Hf(2)	0	0	0.16578 (2)	0.69 (2)
Ba(1)	0	0	$^1/_2$	3.14 (8)
Ba(2)	0	0	0.28839 (3)	1.27 (3)
Ba(3)	0	0	0.39076 (4)	1.28 (3)
S(1)	0	0	0	5.1 (5)
S(2)	0	0	0.1094 (2)	3.8 (3)
S(3)	0	0	0.2203 (2)	2.4 (2)
S(4)	$^1/_4$	$^1/_4$	0.0549 (3)	8.4 (3)
S(5)	$^1/_4$	$^1/_4$	0.1632 (2)	2.1 (1)

[a] Values for anisotropically refined atoms are given in the form of the isotropic equivalent thermal parameter defined as (4/3) $[a^2\beta(1,1) + b^2\beta(2,2) + c^2\beta(3,3) + ab(\cos\gamma)\beta(1,2) + ac(\cos\beta)\beta(1,3) + bc(\cos\alpha)\beta(2,3)]$.

Table V. Selected Bond Distances (Å) and Angles (deg) for $Ba_5Hf_4S_{13}$

Hf(1)–S(1)	2.489 (1)	Ba(1)–S(4)	3.506 (9)
Hf(1)–S(2)	2.47 (1)	Ba(2)–S(3)	3.082 (8)
Hf(1)–S(4)	2.472 (1)	Ba(2)–S(3)	3.523 (1)
Hf(2)–S(2)	2.55 (1)	Ba(2)–S(3)	3.51 (1)
Hf(2)–S(3)	2.470 (8)	Ba(2)–S(5)	3.305 (5)
Hf(2)–S(5)	2.475 (2)	Ba(3)–S(2)	3.50 (6)
Ba(1)–S(1)	3.50 (3)	Ba(3)–S(2)	3.49 (6)
		Ba(3)–S(4)	3.487 (8)
		Ba(3)–S(5)	3.475 (5)
S(1)–Hf(1)–S(2)	180.00	S(2)–Hf(2)–S(3)	180.00
S(1)–Hf(1)–S(4)	89.9 (3)	S(2)–Hf(2)–S(5)	87.3 (2)
S(2)–Hf(1)–S(4)	90.1 (3)	S(3)–Hf(2)–S(5)	92.7 (2)
S(4)–Hf(1)–S(4)	89.76 (1)	S(4)–Ba(1)–S(4)	89.7 (3)
S(5)–Ba(3)–S(5)	90.7 (2)	S(1)–Ba(1)–S(4)	60.03 (8)
S(2)–Ba(3)–S(2)	179.7 (3)	S(1)–Ba(1)–S(4)	120.0 (8)
S(2)–Ba(3)–S(4)	120.3 (2)	S(3)–Ba(2)–S(3)	83.6 (1)
S(2)–Ba(3)–S(5)	120.2 (2)	S(3)–Ba(2)–S(5)	131.6 (1)
S(4)–Ba(3)–S(5)	89.5 (2)	S(5)–Ba(2)–S(5)	96.8 (2)
		S(4)–Ba(3)–S(4)	90.3 (3)

also summarized in Table I. Fractional coordinates and selected bond distances and angles are given in Tables IV and V, respectively.

The structure of $Ba_5Hf_4S_{13}$ consists of $BaHfS_3$ perovskite blocks with corner-sharing HfS_6 octahedra that extend infinitely along a and b and are four layers thick in the c direction (Figure 1). Each four layer block is offset 0 $^1/_2$ 0 relative to the next with double BaS layers separating the blocks. Five of the six Hf–S distances range between 2.489 (1) and 2.470 (8) Å [2.48 Å average] with one long contact between Hf(2) and S(2) of 2.55 (1) Å. The Ba–S contacts to the 12-coordinate Ba atoms inside the perovskite blocks [Ba(1) and Ba(3)] average 3.49 (2) Å. The Ba atoms in the double BaS layers between the blocks [Ba(2)] are 9-coordinate (cf. Ba in Ba_2HfS_4) with Ba–S contacts that range between 3.082 (8) and 3.525 (1) Å which are similar to those found in Ba_2HfS_4 [3.13–3.43 Å].

The structure of $Ba_6Hf_5S_{16}$ (Figure 2) is quite similar to that just described for $Ba_5Hf_4S_{13}$ except the perovskite blocks extend five layers in the c direction. Despite the marginal quality of the structural analysis, the refined structural features seem reasonable and are quite similar to those of $Ba_5Hf_4S_{13}$. The barium atoms in the inner portions of the perovskite blocks [Ba(1) and Ba(2)] are 12-coordinate with typical Ba–S distances of 3.49 (1) Å (average), whereas the contacts to the 9-coordinate Ba atoms in the double BaS layers [Ba(3)] range between 3.09 (2) and 3.516 (2) Å. The Hf–S distances average 2.48 Å and do not show the asymmetries observed in Ba_2HfS_4 [Hf–S = 2.53 (3) and 2.42 (1) Å].

Bond valence analyses[18] of the two phases show consistently high values for the Hf valence states, which range between +4.55 and +4.75. Bond valence analyses for all six perovskite-related Zr and Hf sulfides structurally characterized to date are abnormally high (8–50%) with the largest deviations occurring for the Ba_2MS_4 (M = Zr, Hf) compounds.[11] These deviations may reflect the high degree of compression associated with the K_2NiF_4 type phases.[19]

The new $Ba_{n+1}Hf_nS_{3n+1}$ phases are additional member of the growing class of perovskite-related Ruddlesden–Popper sulfides which have previously received little attention. This class of materials are of interest not only for their "ionic" structure types that contrast with the more common layered chalcogenide phases[2,20] but also due to their similarity in structure and covalency with the high T_c copper oxides where multilayer perovskite type phases predominate.[21] The possibility of superconductivity in

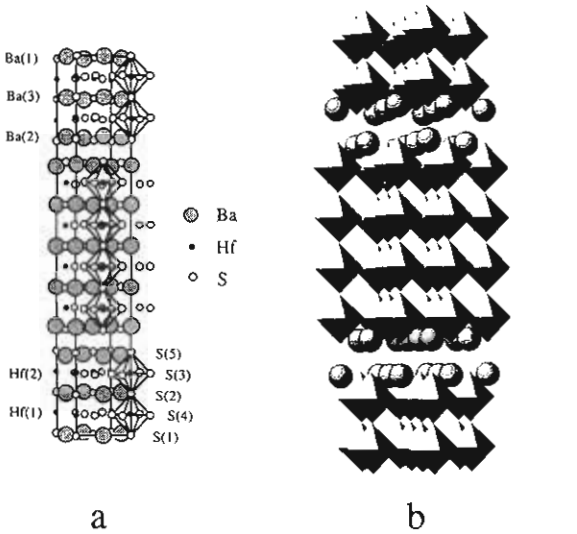

Figure 1. (a) Ball-and-stick representation of the unit cell of $Ba_5Hf_4S_{13}$ showing the relative orientations of the HfS_6 octahedra along c. (b) A polyhedral representation[22] of the HfS_6 octahedra with Ba atoms in the double BaS layers shown as balls. The dimensions of the figure are 2.25a × 2.25b × 1.0c.

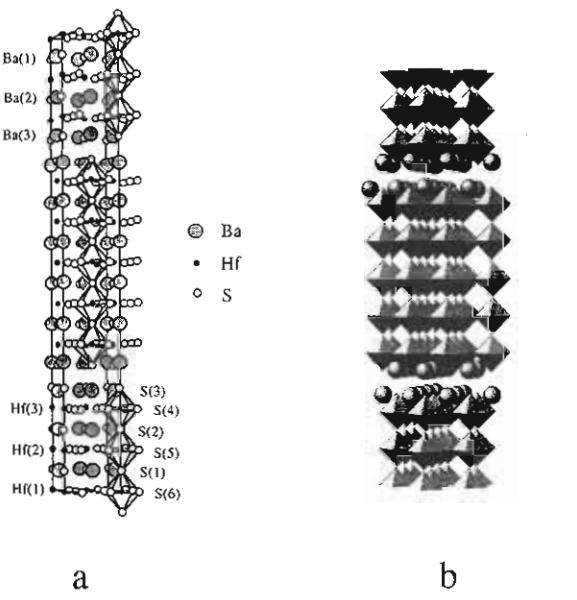

Figure 2. (a) Ball-and-stick representation of the unit cell of $Ba_6Hf_5S_{16}$ showing the relative orientations of the HfS_6 octahedra along c. (b) A polyhedral representation[22] of the HfS_6 octahedra with Ba atoms in the double BaS layers shown as balls. The dimensions of the figure are 2.25a × 2.25b × 1.0c.

(18) Brese, N. W.; O'Keefe, M. *Acta Crystallogr.* **1983**, *B47*, 192.
(19) Ganguly, P.; Rao, C. N. R. *J. Solid State Chem.* **1984**, *53*, 193.
(20) Rao, C. N. R.; Gopalakrishnan, J. *New Directions in Solid State Chemistry*; Cambridge University Press: Cambridge, England, 1986.
(21) Sleight, A. W. *Science* **1988**, *242*, 1519.

doped analogues of these phases is intriguing and is currently under investigation.

Acknowledgment. This work was supported by the National Science Foundation (Grant DMR-8913906), the Exxon Education Foundation, the Center for Superconductivity Research, and Department of Chemistry, University of Maryland. We wish to thank Mr. Cahit Eylem for assistance with the EDAX analysis.

(22) Generated by the CAChe molecular graphics system, Tektronix Inc., Beaverton, OR.

Supplementary Material Available: Text describing the structure determination and tables of crystallographic data, anisotropic thermal parameters, and complete bond distances and bond angles (29 pages); listings of calculated and observed structure factors (5 pages). Ordering information is given on any current masthead page.

Contribution from the Departments of Chemistry, University of California at San Diego, La Jolla, California 92093-0506, and University of Louisville, Louisville, Kentucky 40292, and Microcalorimetry Research Center, Faculty of Science, Osaka University, Toyonaka, Osaka 560, Japan

Valence Detrapping in Mixed-Valence Biferrocenes: Evidence for Phase Transitions†

Robert J. Webb,[1] Paula M. Hagen,[1] Richard J. Wittebort,*[,2] Michio Sorai,*[,3] and David N. Hendrickson*[,1]

Received October 17, 1991

The preparation and physical data characterizing valence detrapping for the PF_6^- and SbF_6^- salts of the mixed-valence 1′,1‴-dichlorobiferrocenium, 1′,1‴-dibromobiferrocenium, and 1′,1‴-diiodobiferrocenium cations are presented. All six compounds are shown to be valence trapped on the vibrational time scale as indicated by C–H bending bands seen in the 815–850-cm^{-1} region of the IR spectrum. ^{57}Fe Mössbauer spectra show that the recrystallized form of the dichloro PF_6^- complex **1** is valence trapped in the 125–350 K range, whereas the initially precipitated form also shows ~50% of a valence-detrapped cation present. Powder XRD data indicate the presence of two different polymorphs of **1**. Only one form of the dibromo PF_6^- complex **2** was found, and it converts from trapped to detrapped in the Mössbauer spectrum at 125 K. Only one polymorph of the diiodo PF_6^- complex **3** was found, and it is valence trapped in the 125–350 K range. Recrystallized dichloro SbF_6^- complex **4** does convert from trapped at low temperatures to detrapped above ~250 K, whereas dibromo SbF_6^- complex **5** remains trapped throughout 125–350 K. Detailed data are presented to show that there are two different polymorphs of diiodo SbF_6^- complex **6**. Mössbauer data show the rapidly precipitated form valence detraps at ~140 K, whereas the recrystallized form detraps at ~270 K. The EPR spectra and powder XRD patterns are different for the two polymorphs. The heat capacity of a 12.2514-g sample of the rapidly precipitated form was determined to show one C_p peak at 134 K, with a small peak at ~270 K attributable to ~5% of the second polymorph. The 134 K phase transition for the metastable polymorph was characterized to have ΔH = 740 ● 50 J mol^{-1} and ΔS = 6.0 ± 0.5 J K^{-1} mol^{-1}. Thus, it is shown that the valence detrapping in the metastable polymorph occurs in a phase transition, where the observed entropy gain (ΔS) is quite close to a value of $\Delta S = R \ln 2$ (=5.76 J K^{-1} mol^{-1}) expected for the mixed-valence 1′,1‴-diiodobiferrocenium cations converting from being trapped in one vibronic state to dynamically interconverting between two vibronic states. Solid-state ^{19}F NMR data for a nonrotating sample of the stable (i.e., recrystallized) polymorph of complex **6** show that the SbF_6^- anion converts from being static at 125 K to rapidly reorientating in the 225–300 K range. Valence detrapping in the mixed-valence 1′,1‴-diiodobiferrocenium cation occurs in the same temperature range as the onset of motion of the SbF_6^- anion.

Introduction

Very recently it has been shown that the solid-state environment about a mixed-valence complex plays a dominant role in determining the rate of intramolecular electron transfer.[4] Some of the most detailed results have been reported for triangular mixed-valence complexes of the composition $[Fe_3O(O_2CCH_3)_6(L)_3]S$, where L is a ligand such as H_2O or (substituted) pyridine and S is a solvate molecule.[5,6] The positioning of ligand substituents on L and solvate molecule S and whether they are static or dynamic in the solid state control the rate of intramolecular electron transfer. It is clear from ^{57}Fe Mössbauer and ^2H NMR data that all of these complexes have a trapped-valence $Fe^{III}_2Fe^{II}$ description at low temperatures. From variable-temperature IR studies[5h,6,7] it is also known that from 50 to 350 K all of these complexes have a trapped-valence $Fe^{III}_2Fe^{II}$ description on the 10^{-11}–10^{-12}-s time scale. At all temperatures the ground-state potential-energy surface for each complex has three or four minima, where at low temperatures the energies of these three or four minima are not the same. One vibronic minimum has the lowest energy, and the Fe_3O complex is valence-trapped in this minimum.

As the crystal is heated, the environment about each $Fe^{III}_2Fe^{II}$ complex tends to become of higher symmetry. The potential-energy surface for the ground state is symmetrized, and the energies of the three or four vibronic states become equal. There are still appreciable potential-energy barriers for a complex to interconvert between the $Fe_a^{III}Fe_b^{III}Fe_c^{II}$ and $Fe_a^{II}Fe_b^{III}Fe_c^{III}$ vibronic states, for example. However, at the higher temperatures the Fe_3O complexes will have enough thermal energy to overcome the potential-energy barriers and interconvert between its three

† Contribution No. 51 from the Microcalorimetry Research Center, for the calorimetric part of this paper.

(1) University of California at San Diego.
(2) University of Louisville.
(3) Osaka University.
(4) (a) Hendrickson, D. N. In *Mixed Valency Systems: Applications in Chemistry, Physics and Biology*; Prassides, K., Ed.; Kluwer Academic Publishers: Dordrecht, The Netherlands, 1991; pp 67–90. (b) Webb, R. J.; Dong, T.-Y.; Pierpont, C. G.; Boone, S. R.; Chadha, R. K.; Hendrickson, D. N. *J. Am. Chem. Soc.* **1991**, *113*, 4806–4812. (c) Webb, R. J.; Geib, S. J.; Staley, D. L.; Rhinegold, A. L.; Hendrickson, D. N. *J. Am. Chem. Soc.* **1990**, *112*, 5031–5042.
(5) (a) Jang, H. G.; Geib, S. J.; Kaneko, Y.; Nakano, M.; Sorai, M.; Rheingold, A. L.; Montez, B.; Hendrickson, D. N. *J. Am. Chem. Soc.* **1989**, *111*, 173. (b) Kaneko, Y.; Nakano, M.; Sorai, M.; Jang, H. G.; Hendrickson, D. N. *Inorg. Chem.* **1989**, *28*, 1067. (c) Oh, S. M.; Wilson, S. R.; Hendrickson, D. N.; Woehler, S. E.; Wittebort, R. J.; Inniss, D.; Strouse, C. E. *J. Am. Chem. Soc.* **1987**, *109*, 1073. (d) Woehler, S. E.; Wittebort, R. J.; Oh, S. M.; Kambara, T.; Hendrickson, D. N.; Inniss, D.; Strouse, C. E. *J. Am. Chem. Soc.* **1987**, *109*, 1063. (e) Woehler, S. E.; Wittebort, R. J.; Oh, S. M.; Hendrickson, D. N.; Inniss, D.; Strouse, C. E. *J. Am. Chem. Soc.* **1986**, *108*, 2938. (f) Hendrickson, D. N.; Oh, S. M.; Dong, T.-Y.; Kambara, T.; Cohn, M. J.; Moore, M. F. *Comments Inorg. Chem.* **1985**, *4*, 329. (g) Sorai, M.; Kaji, K.; Hendrickson, D. N.; Oh, S. M. *J. Am. Chem. Soc.* **1986**, *108*, 702. (h) Cannon, R. D.; White, R. P. *Prog. Inorg. Chem.* **1988**, *36*, 195–298.
(6) (a) Meesuk, L.; Jayasooriya, U. A.; Cannon, R. D. *J. Am. Chem. Soc.* **1987**, *109*, 2009. (b) Johnson, M. K.; Cannon, R. D.; Powell, D. B. *Spectrochim. Acta* **1982**, *38A*, 307.
(7) Oh, S. M.; Hendrickson, D. N.; Hassett, K. L.; Davis, R. E. *J. Am. Chem. Soc.* **1985**, *107*, 8009–8018.

0020-1669/92/1331-1791$03.00/0